Journal of Alzheimer's Disease 26 (2011) 485–494
DOI 10.3233/JAD-2011-102112
IOS Press

Amyloid-β Aggregation on Model Lipid Membranes: An Atomic Force Microscopy Study

Francis Hane[a,1], Elizabeth Drolle[a,1], Ravi Gaikwad[b], Erin Faught[a] and Zoya Leonenko[a,b,*]
[a]*Department of Biology, University of Waterloo, Waterloo, Canada*
[b]*Department of Physics and Astronomy, University of Waterloo, Waterloo, Canada*

Handling Associate Editor: Juan Jimenez

Accepted 19 April 2011

Abstract. Amyloid fibril formation is generally associated with many neurodegenerative disorders, including Alzheimer's disease (AD). Although fibril plaque formation is associated with biological membranes *in vivo*, the role of the cell surfaces in amyloid fibril formation and the molecular mechanism of amyloid toxicity are not well understood. Understanding the details of amyloid interaction with lipid membrane may shed light on the mechanism of amyloid toxicity. Using atomic force microscopy, we investigated aggregation of amyloid-$\beta_{1\text{-}42}$ ($A\beta_{1\text{-}42}$) on model phospholipid membranes as a function of time and membrane composition. Neutral, 1,2-dipalmitoyl-sn-glycero-3-phosphocholine (DPPC) and 1,2-dioleoyl-*sn*-glycero-3-phosphocholine (DOPC), anionic - 1,2-dioleoyl-*sn*-glycero-3-phospho-(1′-*rac*-glycerol) (sodium salt) (DOPG), and cationic - 1,2-dioleoyl-3-trimethylammonium-propane (DOTAP), were used to study the effect of lipid type on amyloid binding. We show that both the charge on the lipid head group and lipid phase affect the interaction of amyloid oligomers with the membrane surface changing the rate of adsorption and causing changes in membrane structure and structure of amyloid deposits. We observed that amyloid aggregates progressively accumulate in a similar manner on the surface of neutral DPPC gel phase membrane and on the surface of fluid phase negatively charged DOPG membrane. In contrast to DPPC and DOPG, positively charged fluid DOTAP membrane and neutral fluid phase DOPC membrane contain amyloid deposits with reduced height, which suggests fusing of $A\beta_{1\text{-}42}$ into the lipid membrane surface.

Keywords: 1,2-dioleoyl-3-trimethylammonium-propane, DOTAP, 1,2-dioleoyl-*sn*-glycero-3-phosphocholine DOPC, 1,2-dipalmitoyl-sn-glycero-3-phosphocholine, DPPC, 1,2-dioleoyl-*sn*-glycero-3-phospho-(1′-*rac*-glycerol), DOPG, Alzheimer's disease, amyloid-$\beta_{1\text{-}42}$, amyloid fibril formation, amyloid-lipid interactions, atomic force microscopy

Supplementary data available online: http://www.j-alz.com/issues/26/vol26-3.html#supplementarydata01

INTRODUCTION

Alzheimer's disease (AD) is a progressive neurological disease that is characterized by dementia, memory loss, and mental degradation believed to be associated with neuronal amyloid plaques. The primary constituent of these amyloid plaques is the amyloid-β (Aβ) peptide, which is cleaved from the amyloid-β protein precursor (AβPP) [1]. Normally, Aβ is in an α-helical form [2] but can misfold into β sheets and aggregate leading to the formation of amyloid oligomers or fibrils. No clear reason as to the cause of this misfolding has been identified [3]. The cascading process leading from an α-helical native protein to mature amyloid fibrils runs through several possible oligomeric intermediate structures. Recent research indicates that these intermediate oligomers have higher neurotoxicity than the more inert mature amyloid fibrils [4–8].

[1]These two authors made equal contributions to this publication.

*Correspondence to: Zoya Leonenko, Department of Physics and Astronomy, University of Waterloo, 200 University Ave, Waterloo, ON, N2 L 3G1, Canada. Tel.: (519) 888-4567, ex. 38273; E-mail: zleonenk@uwaterloo.ca.

ISSN 1387-2877/11/$27.50

Although fibril plaque formation is associated with biological membranes *in vivo*, the majority of research has been done on amyloid fibril formation in solution, where the role of membrane surfaces has not been considered [9–12]. Therefore, despite recent research efforts, the exact mechanism of Aβ interactions with lipid membranes is still not well understood [13]. Several studies reported in the last few years demonstrated that Aβ peptide when reconstituted into the model lipid membrane may form ion pores or channels in membrane bilayers [14–16] and increase the membrane fluidity [17] as well as induce the thinning and reduce the conductance of the cell membrane [18]. In addition, factors such as lipid rafts, cholesterol, pH, and salt have been shown to affect amyloid fibril formation [19–25]. Previously, several groups focused their efforts on elucidating the role of interactions of various Aβ peptides with model lipid membrane and monolayers. Bokvist and colleagues [26] suggested two methods in which Aβ interacts with lipid membranes: binding of monomeric peptide to the lipid membrane and insertion of peptide into the lipid membrane, and hypothesized that the interplay between electrostatic and hydrophobic interaction will drive these processes. Their results suggested pathological interactions of Aβ with neuronal membranes might not only depend on the oligomerization state of the peptide, but also on the type and nature of the supramolecular Aβ–membrane assemblies [26]. Previous research on lipid monolayers have also shown the importance of electrostatic interactions between negatively charged lipids and Aβ peptide at the air water interface [27–29]. Ege et al. [28] have shown that aggregation of $A\beta_{1\text{-}40}$ can take place at considerably lower concentrations when exposed to phospholipid monolayers at the air-water interface, as compared to bulk peptide in solution. Earlier research has shown that the interaction of Aβ with lipid membrane is the initial step of amyloid fibril formation in AD brain [30] and *in vitro* [31, 32].

The phase of the lipid membrane may also play an important role when interactions of Aβ with lipid membrane are considered. A key feature of a membrane, which is defined by the lipid phase, is its relative fluidity (i.e., mobility) of the lipid molecules within the membrane [33]. The major four lipid phases are classified as following: the Lo (liquid ordered); the Lα (liquid-disordered); the gel phase, (Lβ) [33, 34]. The fluidity of the lipid membrane defines the membrane melting transitions [35] and has an important impact on membrane. The phase of the lipid membrane may also be a defining feature for the interaction of amyloid forming peptides. It has been reported recently that fluorescently labeled $A\beta_{1\text{-}42}$ binds preferentially to the gel phase domains in the mixed DPPC/DOPC bilayer [22], although the fibril formation was inhibited by the fluorescent label attached to $A\beta_{1\text{-}42}$ peptide.

In this work, we used Atomic Force Microscopy to elucidate the effect of lipid composition (headgroup charge and phase) on interaction of $A\beta_{1\text{-}42}$ with supported lipid bilayers.

MATERIALS AND METHODS

Lipid bilayer preparation

1, 2-dipalmitoyl-*sn*-glycero-3-phosphocholine (DPPC), 1, 2-dioleoyl-*sn*-glycero-3-phospho-(1′-*rac*-glycerol) (sodium salt) (DOPG), 1,2-dioleoyl-*sn*-glycero-3-phosphocholine (DOPC), and 1,2-dioleoyl-3-trimethylammonium-propane (DOTAP) lipids were purchased from Avanti Polar Lipids (Alabaster AL) in powder form. Lipid vesicle solution was prepared by adding 0.5 mg of dry lipid in 1 mL of ultrapure water. The lipid solution was stirred for 15 min, followed by 10 min of ultrasonic sonication. This stirring/sonication procedure was repeated until the lipid solution was clear which indicated vesicle formation. In order to produce planar supported bilayer 100 μL of vesicle solution was placed on freshly cleaved mica. Vesicles were allowed to fuse for 10–15 min to achieve full bilayer coverage. The sample was washed with ultrapure water to remove unbound vesicles, leaving supported lipid bilayer on mica. Samples of each lipid bilayer (DPPC, DOPC, DOPG and DOTAP) were imaged with the atomic force microscope in liquid to ensure uniformity of the bilayer. One sample of each lipid was rinsed hard with a stream of ultrapure water, causing "nanoholes" in the lipid bilayer. When imaged with the AFM, these samples with holes showed a bilayer height of approximately 5 nm indicating formation of a lipid bilayer.

Amyloid-β incubation

$A\beta_{1\text{-}42}$ was purchased from rPeptide Inc. (Bogart, GA). To ensure the monomeric form of the peptide the peptide was treated according to the Fezoui procedure [36]. 1 mL of HEPES buffer (50 mM, pH 7.8) was added to a 0.5 mg vial of $A\beta_{1\text{-}42}$. The solution was sonicated for 1 minute as directed by rPeptide instructions. 100 μL of $A\beta_{1\text{-}42}$ solution was placed on the lipid bilayers and allowed to incubate at room temperature for the defined time periods of 1 h, 6 h, and 24 h. At the conclusion of incubation time, excess pep-

tide was gently rinsed 3 times with 50 μL of ultrapure water. Nanopure water was added in sufficient quantity to cover the mica slide for imaging with the atomic force microscope.

Atomic force microscopy imaging

Atomic force microscopy (AFM) is a nanoscale imaging technique, which employs a sharp probe scanning over a sample surface and allows for imaging the topographical features at the nanoscale and single molecule level in liquid at near physiological conditions. Samples with supported bilayers were placed in the AFM liquid cells as provided by JPK Instruments AG and Agilent Technologies. The liquid cells were filled with nanopure water, covering the entire sample. All samples were imaged in liquid using a tapping mode (JPK), or MacMode (Agilent) at lower set point to ensure gentle imaging which did not destroy our membrane samples. Veeco DNP-S cantilevers (spring constant 0.5–0.6 N/m) or Agilent Type II Mac Levers (spring constant 2.8 N/m) were used for imaging. Images were scanned at a line rate of 0.5 Hz. Instrument settings were optimized for image quality.

Image analysis

Images were processed with Gwyddion image processing software or JPK image processing software. Images were leveled by subtracting a polynomial fit from the images, and some images were adjusted using the MinMax z-range and a low pass filter to improve image quality.

Statistical analysis

Statistical analysis of oligomer volume has been done using Image Metrology's SPIP software version 5.1.5. The larger fibrils and were neglected. The images were first corrected globally with an average polynomial fit of order 3 and then to get rid of observable steps between subsequent scan lines, the images were leveled using the LMS fit method of order 3. The images were then used for calculating the net volume of material using the height distribution histogram, which is the integral of the area under the histogram and normalized to the volume per surface area. An example of this process is shown in the supplementary material (Available online: http://www.j-alz.com/issues/26/vol26-3.html#supplementarydata01). Statistical analysis of oligomer height distribution was done using cross-section analysis within JPK images processing software. Several images with at least 100 measurements of oligomers and small protofibrils were used for each sample to determine the average height and height distribution.

RESULTS

To mimic the interaction of Aβ with cell membrane we studied interaction of $A\beta_{1\text{-}42}$ peptide with a supported lipid model membrane. When peptides are placed in close proximity to the lipid membrane several processes may occur: 1) the peptides may interact with each other in solution and form fibrils, 2) the peptide monomers and oligomers may interact with lipid headgroups and assemble onto the lipid surface, resulting in oligomers and small protofibrils bound to the lipid membrane. These processes are shown schematically on Fig. 1.

The first process—aggregation of amyloid peptides in solution—has been studied extensively [9–12]. We also performed this control experiment for comparison. Fig. 2 shows AFM images of the aggregation of $A\beta_{1\text{-}42}$ when peptide was incubated in solution for periods of 1 and 24 h respectively. After incubation, a small droplet was placed on mica substrate for 5 min, gently rinsed with water, dried with nitrogen and imaged in air. At a short time of incubation (1 h) we observe formation of oligomers and small protofibrils (which are defined as a few oligomers linked linearly together to form short fibril [9, 12]), Fig. 2A. As incubation time increases, (24 h) we observe formation of longer mature amyloid fibrils, Fig. 2B.

Next, we formed supported lipid bilayers composed of one of the four types of lipids: with neutral (or zwit-

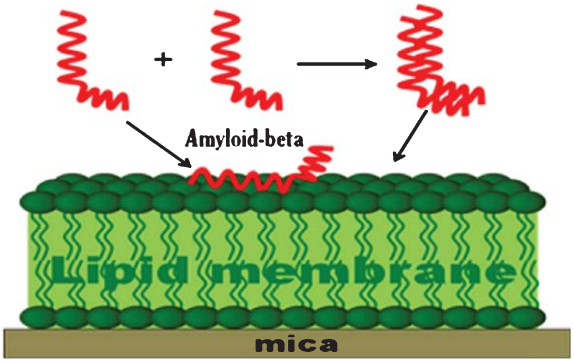

Fig. 1. Schematic, showing a supported bilayer on mica interacting with $A\beta_{1\text{-}42}$ in solution. Two processes may occur: 1) peptides interact with each other and form fibrils in solution; 2) Peptides interact with lipid surfaces (headgroups) and assemble onto the lipid surface.

terionic) head group – DPPC (gel phase) and DOPC (fluid phase), with anionic head group DOPG (fluid phase), and cationic head group DOTAP (fluid phase). Supported lipid bilayers were formed on mica by vesicle fusion, gently rinsed with water to remove the excess of vesicle in solution, and imaged by AFM in liquid. The surfaces of the bilayers were very flat, which is characteristic of lipid bilayers composed of one lipid type. Cross section analysis shows all these surfaces within 400 pm of height differential. A DPPC bilayer with complete coverage is shown on Fig. 3B. To confirm that a bilayer formed on the surface we rinsed the sample hard with a stream of water in order to produce holes in the supported bilayer. Figure 3A shows DPPC bilayer after such rinsing. The dark areas are the mica surface, where the lipid patches were removed by rinsing. The thickness of the bilayer was measured from cross-sections, and was about 5 nm, as expected for the DPPC bilayer measured by AFM.

After a smooth supported bilayer with complete coverage was formed on mica we applied 100 μL of $A\beta_{1\text{-}42}$ solution and incubated peptide solution in a liquid cell with supported bilayer for 10 minutes, and 1, 6, and 24 h. After each time the cell was rinsed gently with water and bilayer with $A\beta_{1\text{-}42}$ deposits was imaged immediately in liquid with AFM. Figure 3C shows AFM image of $A\beta_{1\text{-}42}$ accumulated on a DPPC bilayer after 1 h of incubation. Small round oligomers and short protofibrils were observed, no long mature fibrils were observed at 1 h of incubation for the DPPC bilayer, Fig. 3C. Similar small oligomers and protofibrils growing with time were observed on the surfaces

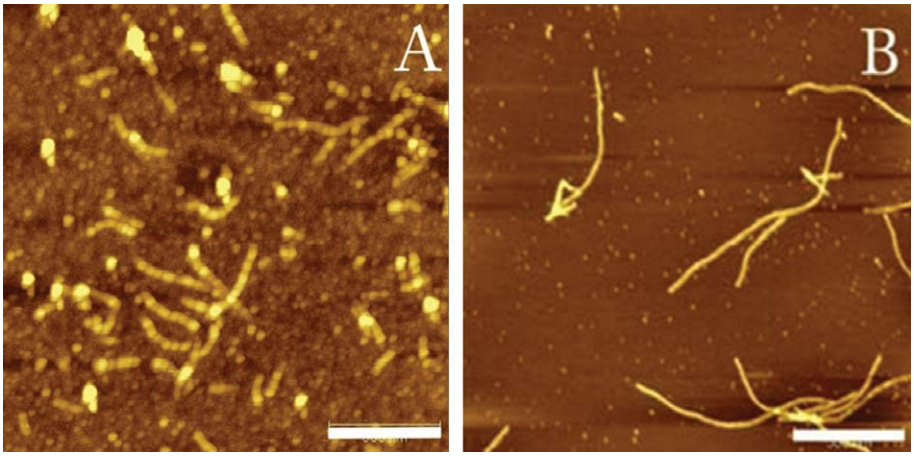

Fig. 2. $A\beta_{1\text{-}42}$, 500 μg/mL in buffer was allowed to incubate in solution. After defined time, 100 μL of solution was deposited on mica for 5 min. After 5 min the mica was rinsed gently to remove excess of solution and imaged with AFM in liquid cell. Scale bar indicates 500 nm. A) Amyloid fibrils formed in solution after1 h of incubation; B) - Amyloid fibrils formed in solution after 24 h of incubation.

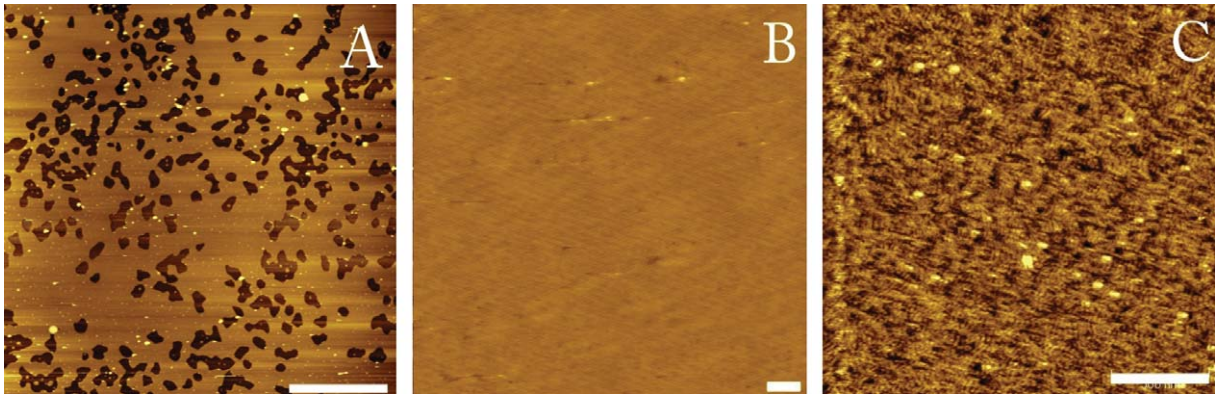

Fig. 3. AFM topography images of DPPC bilayer, A) with holes, after hard rinsing; B) DPPC bilayer with complete surface coverage, after gentle rinsing; C) Aβ deposits on DPPC bilayer with complete surface coverage after 1 h of incubation.

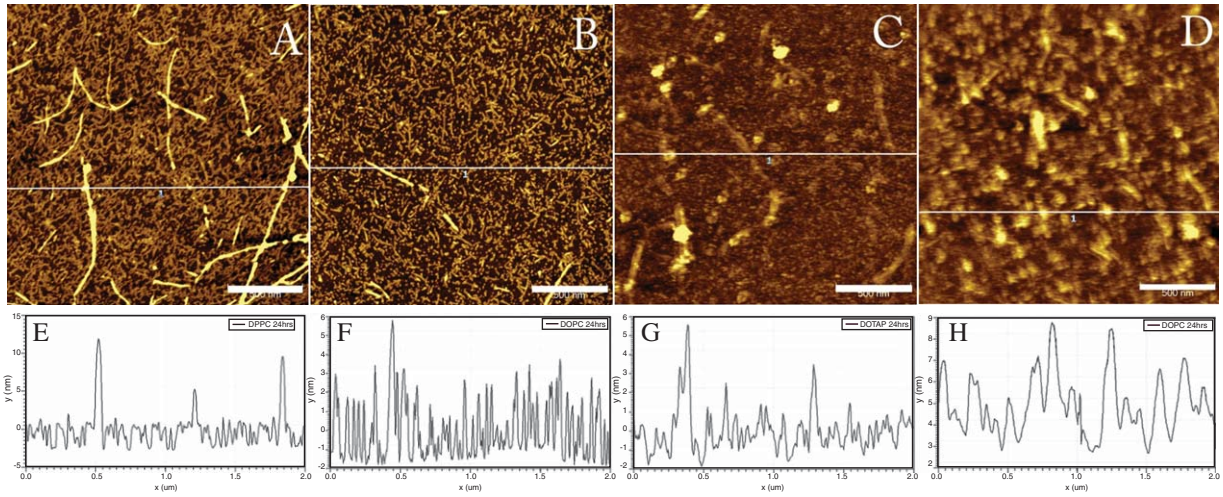

Fig. 4. AFM topography images of Aβ aggregates formed on DPPC (A), DOPG (B), DOTAP (C), and DOPC (D) bilayers after 24 h of incubation. Cross-sections presented underneath the images show the height of protein aggregates measured above the lipid surface, DPPC - (E), DOPG- (F), DOTAP – (G), and DOPC (H). After incubation, bilayers with protein deposits were rinsed gently with water and imaged in liquid cell. Scale bar is 500 nm.

of DOPC, DOTAP and DOPG bilayers (images are not shown). The oligomers have a height 1–3 nm at 1 h incubation, Fig. 3C.

Figure 4 shows formation of $A\beta_{1\text{-}42}$ deposits on supported bilayers after 24 h of incubation imaged by AFM. A DPPC bilayer with amyloid deposits is shown in Fig. 4A. For a DPPC bilayer at 24 h of incubation, we observe accumulation of small oligomers and short protofibrils similar to what we observed at 1 h of incubation, Fig. 3C. In addition, longer twisted fibrils are also visible at 24 h of incubation. The number of oligomers and short fibrils formed on DPPC bilayer surface increases steadily with incubation time, Fig. 5. To account for this we calculated total volume of amyloid deposits accumulated on lipid surfaces (Fig. 5). Larger mature fibrils, presumably formed in solution at 24 h, were excluded from analysis. DPPC bilayer shows accumulation of amyloid deposits – the amyloid deposits volume increases from 1.47 ± 0.08 (10×10^7 nm^3) at 1 h, to 4.07 ± 0.21 at 6 h and slowly increases to 4.55 ± 0.82 at 24 h as seen in Fig. 5.

Statistical analysis of oligomer height distribution was done using cross-section analysis of AFM images, Fig. 5D–F. The results of statistical analysis of oligomer and protofibril height distribution deposited on all lipid bilayers are shown on Fig. 6. For a DPPC supported bilayer the average height of Aβ deposits was changing from 1.15 ± 0.28 nm at 1 h to 4.45 ± 2.80 nm at 24 h of incubation. The length of oligomers and short protofibrils varied from 40 nm to

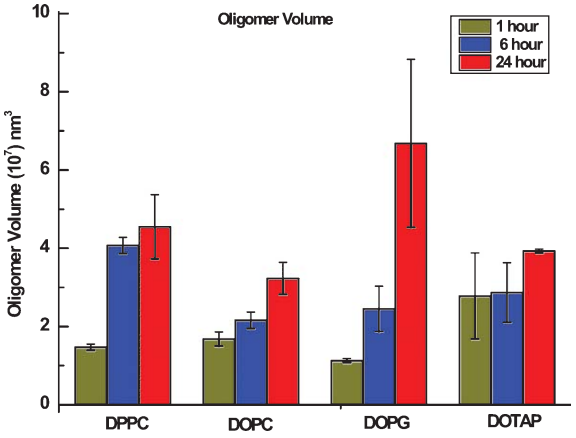

Fig. 5. Statistical analysis of Aβ oligomer volume adsorbed onto supported lipid bilayer DPPC, DOPC, DOPG, and DOTAP respectively at 1 h, 6 h, and 24 h of incubation time. The oligomer volume is calculated on $5 \times 5\ \mu m^2$ scan areas of the bilayers using SPIP software. The process is described in supplementary material.

100 nm. In addition, longer mature fibrils start to form at 24 h of incubation on DPPC bilayer. These larger fibrils have a length up to 2–3 μm and are similar to the fibrils formed in solution at 24 h of incubation, Fig. 2B.

Figure 4B shows AFM topography image of $A\beta_{1\text{-}42}$ deposits on a DOPG bilayer after 24 h of incubation. Similar to what is seen for DPPC (Fig. 4A), we observe that only small mostly round oligomers with a height of 0.97 ± 0.39 nm and short protofibrils (20–300 nm long) formed on the DOPG bilayer surface at 1 h of incubation. After 24 h of incubation, both oligomers

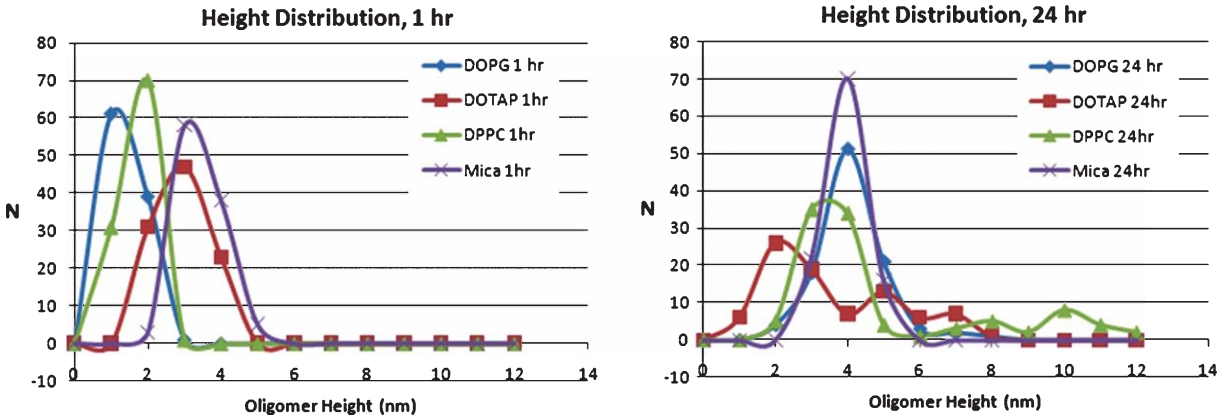

Fig. 6. Height distribution of Aβ oligomers formed on supported lipid bilayers, DPPC, DOPC, DOPG, and DOTAP after 1 h and 24 h of incubation with Aβ peptide solution.

and short protofibrils with a length of 20–300 nm are still present and are well resolved by AFM. The measured height of oligomers and protofibrils increases to 3.60 ± 0.99 at 24 h of incubation. DOPG bilayer shows progressive accumulation of amyloid deposits; the volume increasing from 1.13 ± 0.05 (10×10^7 nm^3) at 1 h, 2.45 ± 0.58 at 6 h and to 6.68 ± 2.15 at 24 h as seen in Fig. 5.

In addition, few mature amyloid fibrils are observed on the very top of the bilayer, at 24 h of incubation, which range in length from 500 nm to 1 μm.

Figure 4C shows AFM topography image of $A\beta_{1\text{-}42}$ deposits formed on DOTAP bilayers after 24 h of incubation. We observe small round oligomers as well as small protofibrils formed on the bilayer surface. The average height of the oligomers formed on DOTAP bilayer after 1 h of incubation is 2.40 ± 0.62 nm and does not change significantly with time (2.99 ± 1.78 nm after 24 h of incubation). Amyloid protofibrils increase in length as incubation time increases from 45–280 nm at 1 h, to 100–580 nm at 24 h of incubation. The volume of amyloid deposits on DOTAP bilayer is the largest at 1 h, 2.78 ± 1.10 (10×10^7 nm^3) compared to other bilayers, remains almost the same at 6 h, 2.87 ± 0.76 and slowly increases to 3.93 ± 0.05 at 24 h as seen in Fig. 5. Longer fibrils with the length of up to 3 μm are also observed. Both oligomers and fibrils are not well resolved and seem to be buried into the bilayer as it is seen from cross-sections and height distributions. We are confident that blurriness of the images is not a result of the poor quality of AFM probe or AFM settings, as high-resolution imaging of nanoparticles and pure bilayers was possible immediately after imaging DOTAP- $A\beta_{1\text{-}42}$ assemblies.

Figure 4D shows AFM topography image of $A\beta_{1\text{-}42}$ deposits on a DOPC bilayer after 24 h of incubation. Similar to what is seen for DOTAP (Fig. 4C), we observe small round oligomers as well as small protofibrils formed on the bilayer surface. The average height of the oligomers formed on DOPC bilayer after 1 h of incubation is measured as 1.81 ± 0.58 nm and changes with time to 3.7 ± 1.45 nm after 24 h of incubation. The volume of amyloid deposits on DOPC membrane progressively increases from 1.68 ± 0.18 (10×10^7 nm^3) at 1 h, 2.16 ± 0.21 at 6 h and to 3.23 ± 0.41 at 24 h as seen in Fig. 5. The average height of the fibrils, measured above the lipid surface is smaller when they are formed on fluid phase DOTAP bilayer (2.99 nm), DOPC bilayer (3.7 nm) and DOPG bilayer (3.60 nm), compared to fibrils formed on mica (4.42 nm) and DPPC bilayer (4.45 nm). Unlike for DPPC and DOPG, the height distribution of oligomers formed on DOPC and DOTAP becomes very wide at 24 h of incubation (Fig. 6).

DISCUSSION

The difference in fibril formation between $A\beta_{1\text{-}42}$-incubated in solution and $A\beta_{1\text{-}42}$ -incubated on lipid bilayers is striking: fibrils formed in solution grow in length with time up to several microns long, Fig. 2, are thin and show twisted morphology, characteristic for fibrils formed in solution [12]. Fig. 2A shows $A\beta_{1\text{-}42}$, which have been incubated in solution for 1 h and deposited on mica. Compared to fibril formation in solution, amyloid aggregation is different on lipid surfaces. When we incubate $A\beta_{1\text{-}42}$ on lipid bilayers, we

observe that small oligomers and short protofibrils are present at all times, while long fibrils, characteristic for incubation in solution, are rarely observed. This suggests higher propensity of oligomers to lipid surfaces compared to mature fibrils, which correlates well with the earlier reported higher neurotoxicity of oligomers compared to fibrils [4–8].

As shown in Figs. 3C and 4A, on DPPC bilayer we observe progressive accumulation of oligomers and short protofibrils on the lipid surface, indicated by an increase in the total volume of amyloid deposits (Fig. 5). The oligomers are well resolved and the height of the deposits measured above the lipid surface increases with the time of incubation, which also indicates accumulation of oligomers and short protofibrils on the surface of DPPC bilayer, Figs. 4A and 6. After 24 h of incubation of $A\beta_{1\text{-}42}$ on the DPPC bilayer, the surface is almost completely and uniformly covered by densely packed oligomers and short protofibrils. Some longer fibrils that we observed at 24 h of incubation on lipid surfaces resemble the long fibrils formed in solution and were likely also formed in solution above the lipid bilayer, and then adsorbed onto the bilayer surface. In the case of DOPG bilayers, oligomer volume increases slowly at 1 h and 6 h (Fig. 5) and increases further at 24 h. Individual oligomers and protofibrils are well resolved by AFM on both DPPC and DOPG bilayers. We observe progressive accumulation of oligomers and short fibrils on the DOPG lipid surfaces, similar to DPPC, Fig. 6. This suggests that $A\beta_{1\text{-}42}$ binds to the lipid surfaces of DPPC and DOPG but does not fuse into the lipid membrane and does not disturb the surface of membrane. Both DPPC and DOPG lipid membrane act as a solid substrate which binds and accumulates $A\beta_{1\text{-}42}$ oligomers without affecting the AFM resolution.

DOTAP lipid surfaces show different behavior. The oligomer volume (Fig. 5) is highest at 1 h compared to other lipid type and saturates at 1 h. After this, it stays nearly the same at later times of incubation (6 h and 24 h). This means that initial binding and accumulation occurs faster on DOTAP bilayer, than on DOPC and DPPC, and the DOPG is the slowest at 1 h, which may indicate the preferable interaction of DOTAP positively charged lipid heads with negatively charged amyloid monomers and oligomers. The height distribution does not increase progressively from 1 h to 24 h, but becomes broader, for DOTAP, Fig. 6. This suggests that $A\beta_{1\text{-}42}$ oligomers may interact differently with DOTAP bilayer, in that they may penetrate into the bilayer headgroup area and disturb the flat surface of the bilayer, instead of simply accumulating on surface as observed on DPPC and DOPG bilayers. This is revealed by AFM images, Fig. 4C, which show no single well-resolved oligomers or protofibrils on DOTAP bilayer, as observed on DPPC and DOPG bilayers, but rather fused clusters which are presumably protein-lipid complexes. This fact suggests stronger interaction between DOTAP lipids and $A\beta_{1\text{-}42}$, compared to other lipid membrane, which changes the uniform flat surface of the bilayer to produce defects in the bilayer. It has been reported earlier that due to high fluidity and electrostatic interaction DOTAP lipids have strong interaction with charged DNA, which results into partial penetration of DNA into the bilayer headgroup area [37, 38]. Considering the complex charge distribution and total negative charge for $A\beta_{1\text{-}42}$ monomer at neutral pH the interaction of $A\beta_{1\text{-}42}$ with DOTAP lipids should be stronger and may cause similar bilayer deformation, resulting from clustering of positively charged DOTAP lipids around Aβ deposits. Slower progression of the amyloid deposition at 24 h can be also be explained by the fact that amyloids may neutralize the positive charge at the lipid headgroups upon binding and therefore reduce the electrostatic driving force for further adsorption on the surface.

The DOPC bilayer shows similar behavior as DOTAP in faster accumulation of oligomers in the first 6 h, and slower progression at 24 h, Fig. 5, compared to DPPC and DOPG. Oligomers formed on DOPC are also not well resolved likely due to the partial fusion into the bilayer surface. Both lipid bilayers show wide distribution of oligomer sizes at 24 h. This suggests a stronger interaction of $A\beta_{1\text{-}42}$ with lipid head groups and possible formation of lipid-protein clusters. We can see that all three fluid phase bilayers DOTAP (positive), DOPG (negative), and DOPC (neutral) bind $A\beta_{1\text{-}42}$ effectively but show different degrees of membrane disturbance and a different order of $A\beta_{1\text{-}42}$ deposits on the bilayer. While we observed significant fusion of $A\beta_{1\text{-}42}$ into DOTAP and DOPC bilayers upon binding, (Figs. 4 and 5), we observed binding of $A\beta_{1\text{-}42}$ to the DPPC and DOPG bilayers, but no disturbance of the bilayer. DPPC (gel phase) and DOPC (fluid phase) also show different results, although the charge on the head group is the same. This leads us to conclusion that not only the charge, but also the phase of the lipid membrane affects the interaction of $A\beta_{1\text{-}42}$ with the membrane. Our results correlate with the trend described in monolayers studies [27, 28], indicating that $A\beta_{1\text{-}40}$ interacts with charged lipids, but the insertion of the peptide depends on the compression of the monolayer, which correlates with the bilayer

phase [27]. We observed binding but no incorporation of $A\beta_{1\text{-}42}$ into the DPPC and DOPG bilayer, and disordering of DOTAP and DOPC bilayers, which most likely is a result of partial fusion of the peptide into the lipid head group area upon binding, Figs 4 and 5. Although DOPG and DOTAP bilayers are both fluid at room temperature, we observed more ordered amyloid-lipid assemblies for DOPG membrane than for DOTAP, which correlates with peptide ordering reported on negatively charged monolayers [27]. Importantly, we observed larger membrane disturbance due to penetration of $A\beta_{1\text{-}42}$ into the positively charged DOTAP bilayer than into the negatively charged DOPG bilayer, Fig. 5. This can be explained by the electrostatic interactions that may order the negatively charged peptide on the surface DOPG lipids. Although $A\beta_{1\text{-}42}$ is negatively charged at neutral pH (total charge-3), it has complex distribution of charged and hydrophobic regions, which may result in different orientations of the monomers and oligomers on charged surfaces. Oriented alternating charges may result from the peptide-lipid arrangements on the DOPG membrane surfaces, which in turn may result into the ordering of the lipid phase, therefore reducing the fluidity of DOPG bilayer and degree of disturbance caused by amyloid deposits. Both DOTAP and DOPG bilayers normally exist in fluid phase at room temperature. The fluid-gel transition temperatures for DOPG and DOTAP are –18°C [41] and –11.9°C [42] respectively. The structures of the four lipids are shown in Fig. 7. DOTAP bilayer has smaller head groups that repulse each other due to the positive charge and may be therefore more effectively disrupted by the negatively charged peptide oligomers interacting with the lipid head groups. Comparing neutral DOPC and DPPC bilayers, we can clearly see that the differences in phase produce different interaction with $A\beta_{1\text{-}42}$. DOPC is analogue of DPPC with similar neutral head group, but differs in saturation of the chains and exists in fluid phase at room temperature, while the DPPC is present in gel phase. DOPC bilayer behaves similarly to the fluid phase DOTAP bilayer accumulating broad distribution of oligomer sizes, which likely penetrate into the bilayer head group area, forming lipid-peptide clusters.

This demonstrates that both the phase and the charge of lipid membrane are important for binding and accumulation of $A\beta_{1\text{-}42}$ deposits on the surface of lipid membrane, which in turn may affect the morphology of lipid membrane surface and may lead to altering membrane potential upon amyloid binding.

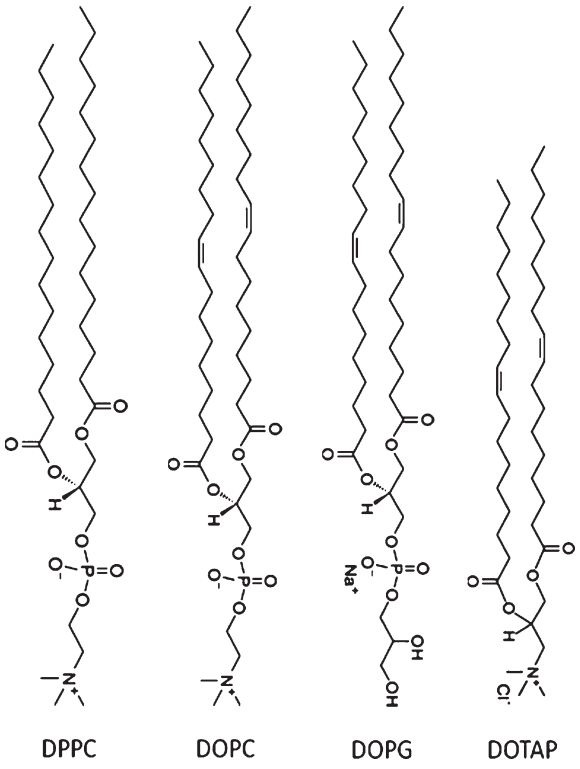

Fig. 7. The structure and charge distribution in the lipid head group for lipids used: DPPC-1, 2-dipalmitoyl-*sn*-glycero-3-phosphocholine, DOPC-1, 2-dioleoyl-*sn*-glycero-3-phosphocholine, DOPG-1, 2-dioleoyl-*sn*-glycero-3-phospho-(1′-*rac*-glycerol) (sodium salt), DOTAP-1, 2-dioleoyl-3-trimethylammonium-propane. The structures are adapted from Avanti Polar Lipids website (http://avantilipids.com), where the lipids were purchased.

CONCLUSION

We studied fibril formation of $A\beta_{1\text{-}42}$ on model supported lipid bilayers composed of positively charged (DOTAP), negatively charged (DOPG), and zwitterionic (DPPC and DOPC) lipids using high resolution atomic force microscopy. AFM images show binding and progressive accumulation of $A\beta_{1\text{-}42}$ oligomers and short protofibrils on the surface of zwitterionic lipid membrane DPPC and negatively charged lipid membrane DOPG. Fluid phase lipid bilayers (DOTAP (positively charged) and DOPC (neutral) show stronger interference with $A\beta_{1\text{-}42}$. Significant disturbance of the lipid membrane for positively charged fluid DOTAP bilayer and neutral fluid DOPC was also observed. This indicates the importance of electrostatic interactions as well as lipid membrane phase in amyloid-membrane interaction, which affect both the structure of amyloid aggregates and the structure of the lipid membrane itself.

ACKNOWLEDGMENTS

The authors thank the Natural Sciences and Engineering Research Council (NSERC) of Canada, Canada Foundation for Innovation (CFI), and Ontario Ministry of Research and Innovation (Ontario Research Fund) for financial support. The authors greatly acknowledge JPK Instruments and Agilent Technologies for their technical support as well as Dr. David Fry for critical reading of the manuscript.

Authors' disclosures available online (http://www.j-alz.com/disclosures/view.php?id=861).

REFERENCES

[1] Kang J, Lemaire HG, Unterbeck A, Salbaum JM, Masters CL, Grzeschik KH, Multhaup G, Beyreuther K, Muller-Hill B, (1987) The precursor of Alzheimer's disease amyloid A4 protein resembles a cell-surface receptor. *Nature* **325**, 733-736.

[2] Kallberg Y, Gustafsson M, Persson B, Thyberg J, Johansson J (2001) Prediction of amyloid fibril-forming proteins. *J Biol Chem* **276**, 12945-12450.

[3] Carrell R (1998) Conformational changes and disease - serpins, prions and Alzheimer's. *Curr Opin Struct Biol* **8**, 799-809.

[4] Lambert MP, Barlow AK, Chromy BA, Edwards C, Freed, Liosatos M, Morgan TE, Rozovsky I, Trommer B, Viola KL, Wals P, Zhang C, Finch CE, Krafft GA, Klein WL (1998) Diffusible, nonfibrillar ligands derived from $A\beta_{1-42}$ are potent central nervous system neurotoxins. *Proc Natl Acad Sci U S A* **95**, 6448-6453.

[5] Kayed R, Head E, Thompson JL, McIntire TM, Milton SC, Cotman CW, Glabe CG (2003) Common structure of soluble amyloid oligomers implies common mechanism of pathogenesis. *Science* **300**, 486-489.

[6] Dahlgren KN, Manelli AM, Stine WB Jr, Baker LK, Krafft GA, LaDu MJ (2002) Oligomeric and fibrillar species of amyloid-β peptides differentially affect neuronal viability. *J Biol Chem* **277**, 32046-32053.

[7] Roher AE, Chaney MO, Kuo YM, Webster SD, Stine WB, Haverkamp LJ, Woods AS, Cotter RJ, Tuohy JM, Krafft GA, Bonnell BS, Emmerling MR (1996) Morphology and toxicity of Aβ-(1–42) dimer derived from neuritic and vascular amyloid deposits of Alzheimer's disease. *J Biol Chem* **271**, 20631-20635.

[8] Campioni S, Mannini B, Pensalfini A, Zampagni M, Parrini C, Evangelisti E, Relini A, Stefani M, Dobson CM, Cecchi C, Chiti F (2010) A causative link between the structure of aberrant protein oligomers and their toxicity. *Nat Chem Biol* **6**, 140-147.

[9] Dobson CM (2001) The structural basis of protein folding and its links with human disease. *Phil Trans R Soc Lond B* **356**, 133-145.

[10] Johansson J (2003) Molecular determinants for amyloid fibril formation: lessons from lung surfactant protein C. *Swiss Med Wkly* **133**, 275-282.

[11] Chiti F, Dobson CM (2006) Protein misfolding, functional amyloid, and human disease. *Annu Rev Biochem* **75**, 333-366.

[12] Blackley HKL, Patel N, Davies MC, Roberts CJ, Tendler SJB, Wilkinson MJ, Williams PM (1999) Morphological development of β(1-40) amyloid fibrils. *Exp Neurol* **158**, 437-443.

[13] Walsh DM, Klyubin I, Fadeeva JV, Rowan MJ, Selkoe DJ (2002) Amyloid-β oligomers: their production, toxicity and therapeutic inhibition. *Biochem Soc Trans* **30**, 552-557.

[14] Lin H, Bhatia I, Ratneshwar LAL (2001) Amyloid β protein forms ion channels: implications for Alzheimer's disease. pathophysiology *FASEB J* **15**, 2433-2444.

[15] Quist A, Doudevski I, Lin H, Azimova R, Ng D, Frangione B, Kagan B, Ghiso J, Lal R (2005) Amyloid ion channels: A common structural link for protein-misfolding disease. *Proc Natl Acad Sci U S A* **102**, 10427-10432.

[16] Arispe N (2004) Architecture of the Alzheimer's AßP Ion Channel Pore. *J Membrane Biol* **197**, 33-48.

[17] Kremer J, Pallitto MM, Sklansky DJ, Murphy RM (2000) Correlation of β-amyloid aggregate size and hydrophobicity with decreased bilayer fluidity of model membranes. *Biochem* **39**, 10309-10318.

[18] Sokolov Y, Kozak J, Kayed R, Chanturiya A, Clabe C, Hall J (2006) Soluble amyloid oligomers increase bilayer conductance by altering dielectric structure. *J Gen Physiol* **128**, 637-647.

[19] Cordy JM, Hooper NM, Turner AJ (2006) The involvement of lipid rafts in Alzheimer's disease. *Mol Membr Biol* **23**, 111-122.

[20] Sharp JS, Forrest JA, Jones RAL (2002) Surface denaturation and amyloid fibril formation of insulin at model lipid-water interfaces. *Biochem* **41**, 15810-15819.

[21] Yip CM, Elton EA, Darabie AA, Morrison MR, McLaurin J (2001) Cholesterol, a modulator of membrane-associated Aβ-fibrillogenesis and neurotoxicity. *J Mol Biol* **11**, 723-734.

[22] Choucair A, Chakrapani M, Chakravarthy B, Katsaras J, Johnston L (2007) Preferential accumulation of Aβ(1-42) on gel phase domains of lipid bilayers: an AFM and fluorescence study. *Biochim Biophys Acta* **1768**, 146-154.

[23] Neugroschl J, Sano M (2010) Current treatment and recent clinical research in Alzheimer's disease. *Mt Sinai J Med* **77**, 3-16.

[24] Curtain C, Ali F, Smith D, Bush A, Masters C, Barnham K (2003) Metal ions, pH, and cholesterol regulate the interactions of Alzheimer's disease amyloid-beta peptide with membrane lipid. *J Biol Chem* **278**, 2977-2982.

[25] Cruz L, Urbanc B, Borreguero JM, Lazo ND, Teplow DB, Stanley HE (2005) Solvent and mutation effects on the nucleation of amyloid-protein folding. *Proc Natl Acad Sci U S A* **102**, 18258-18263.

[26] Bokvist M, Lindström F, Watts A, Grobner G (2004) Two types of Alzheimer's β-amyloid (1–40) peptide membrane interactions: aggregation preventing transmembrane anchoring versus accelerated surface fibril formation. *J Mol Biol* **335**, 1039-1049.

[27] Maltseva E, Kerth A, Blume A, Mçhwald A, Brezesinski G (2005) Adsorption of amyloid β (1–40) peptide at phospholipid monolayer. *Chem Biol Chem* **6**, 1817-1824.

[28] Ege C, Majewski J, Wu G, Kjaer K, Lee KY (2005) Templating effect of lipid membranes on Alzheimer's amyloid beta peptide. *Chemphyschem* **6**, 226-229.

[29] Ionov M, Klajnert B, Gardikis K, Hatziantoniou S, Palecz B, Salakhutdinov B, Cladera J, Zamaraeva M, Demetzos C, Bryszewska M (2010) Effect of amyloid beta peptides Aβ1–28 and Aβ25–40 on model lipid membranes. *J Therm Anal Calorim* **99**, 741-747.

[30] Yanagisawa K, Odaka A, Suzuki N, Ihara Y (1995) GM1 ganglioside bound amyloid β-protein (Aβ): a possible form of preamyloid in Alzheimer's disease. *Nat Med* **1**, 1062-1066.
[31] Terzi E, Holzemann G, Seelig J (1995) Self-association of beta-amyloid peptide (1-40) in solution and binding to lipid membranes. *J Mol Biol* **252**, 633-642.
[32] Choo-Smith LP, Surewicz WK (1997) The interaction between Alzheimer amyloid β (1-40) peptide and ganglioside GM1-containing membranes. *FEBS Lett* **402**, 95-98.
[33] Feigenson GW (2006) Phase behavior of lipid mixtures. *Nature Chem Biol* **2**, 560-563.
[34] Lingwood D, Simons K (2010) Lipid rafts as a membrane-organizing principle. *Science* **327**, 46-50.
[35] Koynova R, Caffrey M (2002) An index of lipid phase diagrams. *Chem Phys Lipids* **115**, 107-219.
[36] Fezoui Y, Hartley D, Harper J, Khurana R, Walsh D, Condron M, Selkoe D, Lansbury P, Fink A, Teplow D (2000) An improved method of preparing the amyloid p-protein for fibrillogenesis and neurotoxicity experiments. *Amyloid: Int J Exp Clin Invest* **7**, 166-178.
[37] Leonenko Z, Finot E, Ma H, Dahms T, Cramb D (2004) Investigation of temperature induced phase transitions in DOPC and DPPC phospholipid bilayers using temperature-controlled scanning force microscopy. *Biophys J* **86**, 3783-3793.
[38] Leonenko Z, Cramb D (2002) Effect of DNA adsorption on the phase cycling of a supported phospholipid bilayer. *Nanoletters* **2**, 305-309.
[39] Seelig A (1987) Local anesthetics and pressure: a comparison of dibucaine binding to lipid monolayers and bilayers. *Biochim Biophys Acta* **899**, 196-204.
[40] Wu J, Siu SF (2002) Study of β-amyloid insertion into phospholipid membranes using monolayer technique. *J Biol Chem* **67**, 1283-1288.
[41] Silvius J (1982) Thermotropic phase transitions of pure lipids in model membranes and their modifications by membrane proteins. In: Lipid-Protein Interactions, John Wiley & Sons, Inc., New York.
[42] Regelin A (2000) Biophysical and lipofection studies of DOTAP analogs. *Biochim Biophys Acta* **1464**, 151-164.